RevMexAA (Serie de Conferencias), **12**, 106–111 (2002)

PLANETARY NEBULAE RESULTS FROM THE *INFRARED SPACE OBSERVATORY*[1]

R. H. Rubin,[2,3] R. J. Dufour,[4] S. W. J. Colgan,[2] A. Liao,[2] J. P. Harrington,[5] D. A. Levine,[6] and S. D. Lord[6]

RESUMEN

Las observaciones con el *Observatorio Espacial Infrarrojo* (*ISO*) proveen medios para obtener importantes propiedades del plasma en nebulosas gaseosas, incluyendo a las nebulosas planetarias (NPs). Presentamos algunos resultados de densidades electrónicas promedio, determinadas de los cocientes de flujo de varias líneas IR de estructura fina. Dado que la apertura espectroscoópica de *ISO* fué siempre $\geq 14'' \times 20''$, estas densidades representan medidas macroscópicas de nuestra muestra de NPs. Encontramos algunos casos donde el cociente de flujos observados está claramente fuera del intervalo de predicciones teóricas de los datos atómicos usuales. En estos casos, los datos de *ISO* no pueden usarse para derivar densidades electrónicas, sino que dan indicaciones de como mejorar los datos atómicos para las fuerzas de colisión.

ABSTRACT

Observations with the *Infrared Space Observatory* (*ISO*) provide a means to assess important properties of the plasma in gaseous nebulae, including planetary nebulae (PNs). We present some results for average electron densities that have been determined from the flux ratios of several fine-structure, infrared emission lines. Because the *ISO* spectroscopic aperture was always at least as large as $14'' \times 20''$, these represent macroscopic measurements for our sample of PNs. We find some instances of the observed line flux ratio being clearly out of range of the theoretical predictions using current atomic data. In these cases, the *ISO* data cannot presently be used with these atomic data to derive electron density, but rather provide direction for needed improvements in the atomic collision strengths.

Key Words: **ISM: STRUCTURE — PLANETARY NEBULAE: GENERAL**

Ionized Gaseous Nebulae (Mexico City, 21-24 November 2000)
Editors: William Henney, José Franco, Marco Martos, & Miriam Peña

1. INTRODUCTION

Most observational tests of the chemical evolution of the universe rest on emission line objects; these define the endpoints of stellar evolution and probe the current state of the interstellar medium. Gaseous nebulae are laboratories for understanding physical processes in all emission-line sources, and probes for stellar, galactic, and primordial nucleosynthesis.

There is a fundamental issue that continues to be problematic—the discrepancy between heavy element abundances inferred from emission lines that are collisionally excited compared with those that are due to recombination/cascading—the so-called "recombination lines". We shall refer to this as "the abundance dichotomy". Studies of planetary nebulae (PNs) contrasting recombination and collisional abundances (Liu et al. 1995; Kwitter & Henry 1998) often find differences exceeding a factor of two and even as large as 15 in NGC 4361 (Liu 1998). In an extensive study of the PN NGC 6153, Liu et al. (2000) found that C^{++}/H^+, N^{++}/H^+, O^{++}/H^+, and Ne^{++}/H^+ ratios derived from optical recombination lines are all a factor of ~ 10 higher than the corresponding values deduced from collisionally-excited lines. Abundances determined from these two methods disagree by a factor larger than that representing the spread of abundances used to determine such fundamental quantities as galactic abundance gradients (e.g., Shaver et al. 1983; Simpson et al. 1995; Henry & Worthey 1999).

Most of the efforts to explain the abundance dichotomy have attempted to do so by examining electron temperature (T_e) variations in the plasma. This is often done, using the formalism of Peimbert (1967), in terms of the mean-square variation (t^2) of T_e. The inferred metallicity obtained by using the usual (optical/UV) forbidden lines is very sensitive to T_e (exponential) and t^2. On the other hand, recombination lines are rather insensitive to T_e and t^2.

[1]Based on observations with *ISO*, an ESA project with instruments funded by ESA Member States (especially the PI countries: France, Germany, the Netherlands and the United Kingdom) with the participation of ISAS and NASA. This research was supported in part by *ISO* Data Analysis funding from NASA.

[2]NASA/Ames Research Center. [3]Orion Enterprises.
[4]Rice University. [5]University of Maryland.
[6]IPAC, California Institute of Technology.

Ionized Gaseous Nebulae (Mexico City, 21-24 November 2000)
Editors: William Henney, José Franco, Marco Martos, & Miriam Peña

This has been extensively reviewed in other papers in this Conference and the Proceedings. It seems clear that something more than T_e variations is necessary to explain the abundance dichotomy.

Here we address other ingredients that may affect the determination of elemental abundances from observations. Perhaps the most important of these is density variations. While T_e variations are expected theoretically to be fairly small in PNs and H II regions, variations in N_e are almost certainly very large. High N_e values are inferred in the cometary knots of the Helix nebula ($\sim 10^3$ cm^{-3}, e.g., Walsh & Meaburn 1993; Burkert & O'Dell 1998) and around proplyds in Orion ($\sim 10^6$ cm^{-3}, e.g., Henney & O'Dell 1999 and references therein). Gas at $N_e = 10^6$ cm^{-3} will produce 10^6 times as much emission as say "normal" nebular gas at $N_e = 10^3$ cm^{-3} for recombination lines and collisionally-excited lines that are not suffering collisional deexcitation—when $N_e < N_{crit}$ (the critical density).

Several well known line ratios of collisionally-excited lines serve as diagnostics of N_e, probing different ionization conditions and different density regimes. Because various collisionally-excited lines undergo collisional deexcitation at different N_{crit} values, to derive an average N_e for a given line ratio depends on the specific N_e (and T_e) dependence of the respective volume emissivities. In general, different average N_e values are obtained for various line pairs due to different contributions to the observed intensities from the volume observed. Very substantial biases in the inference of abundances from collisionally-excited lines may then result (Rubin 1989; Viegas & Clegg 1994; Liu et al. 2000).

2. THE PROMISE OF THE INFRARED FOR DENSITY DIAGNOSTICS

Measurement of the two $\Delta J = 1$ far-infrared (FIR) fine-structure transitions for species with a ^{3}P ground state provides a diagnostic for N_e. The ratio of their fluxes is a sensitive indicator of N_e (over some range in N_e) that generally is not significantly affected by T_e or extinction. For example, the flux ratios [O III] 52/88 μm, [S III] 19/33 μm, and [N II] 122/205 μm provide N_e[O III], N_e[S III], and N_e[N II], respectively, as shown in Figure 1 (Rubin et al. 1994).

There is only a weak dependence on T_e as illustrated for each species by the three curves for $T_e = 5000$, 8000, and 10 000 K. For conditions prevalent in many PNs and H II regions, these lines readily show the effect of collisional deexcitation because some of the plasma may exceed their respective N_{crit}-values. We are able to use only two of the above

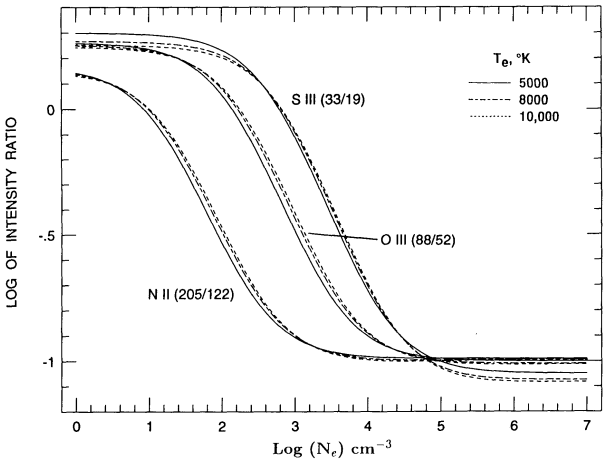

Fig. 1. Three valuable indicators of N_e—the intensity ratio of [N II] (205/122), [O III] (88/52), and [S III] (33/19) vs. N_e (cm^{-3}). The [N II] ratio is most sensitive at the lowest N_e, and [S III] at the highest N_e.

diagnostics because *ISO* did not observe the 205 μm line.

With *ISO*, there are now at least three important additional IR line ratios—[Ne III] 36.0/15.5 μm, [Ne V] 14.3/24.3 μm, and [Ar III] 21.8/8.99 μm—available for studies of N_e structure and variations. This is because ISO was able to observe the [Ne III] 15.5 μm, [Ne V] 14.3 μm, and [Ar III] 21.8 μm lines, which suffer very seriously from the atmosphere even for airborne astronomy, e.g., for the Kuiper Airborne Observatory (KAO) or SOFIA. (Observations of these lines with the *IRAS* LRS were sparse and of dubious quality.) These three ratios are sensitive indicators of higher density material than are the other three ratios mentioned earlier. Two of these ratios—[Ne III] 36/15 μm and [Ar III] 22/9 μm—are displayed in Figure 2.

Both ratios are similar in that they are most discriminant in the range $3.8 \lesssim \log N_e \lesssim 5.4$. We will use two more N_e-diagnostic line ratios [Mg V] 13.5/5.61 μm and [Ar V] 13.1/7.9 μm. These will be used to probe the higher ionization gas. Although usually weaker than those lines mentioned earlier, all are expected to be seen in a large number of high ionization PNs. The hope of the *ISO* IR data is that these numerous "new" N_e diagnostics, in combination with those N_e diagnostics available from the optical/UV, will permit a viable tomographic analysis of the N_e structure in PNs.

3. *ISO* OBSERVATIONS AND ANALYSIS

Under our GO programs, we observed the PNs NGC 2022, NGC 6210, NGC 6818, and IC 2165 with the *ISO* Short Wavelength Spectrometer (SWS). Our observations with SWS were made in SWS02

Ionized Gaseous Nebulae (Mexico City, 21-24 November 2000)
Editors: William Henney, José Franco, Marco Martos, & Miriam Peña

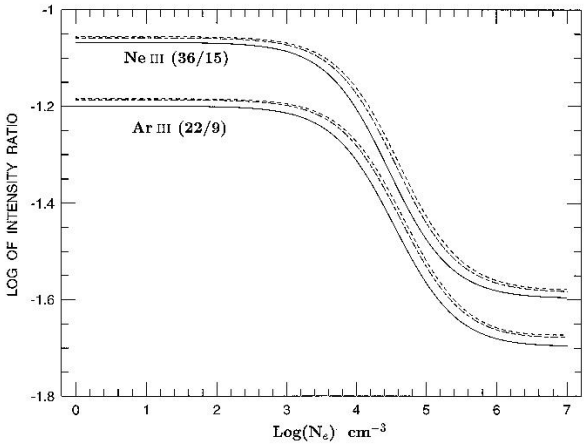

Fig. 2. Similar to Fig. 1 for two other outstanding indicators of N_e—the intensity ratio of [Ne III] (36/15) and [Ar III] (22/9). These diagnostics are now available from *ISO*. These ratios are sensitive indicators of higher density material than those ratios in Fig. 1.

mode, which provides higher spectral resolution than SWS01 mode. One of our goals was to derive N_e from several diagnostic line pairs in order to address density variations within these objects. As described above, we aimed to obtain N_e values from the following six flux ratios: [Ne III] (15.5/36.0 μm), [Ne V] (14.3/24.3), [Mg V] (5.61/13.5), [S III] (18.7/33.5), [Ar III] (8.99/21.8), and [Ar V] (7.90/13.1). Because the *ISO*/SWS aperture size depends on wavelength, the above line fluxes are not always directly comparable. For the lines discussed here, the sizes were: $14'' \times 20''$ for the 5.61, 7.90, & 8.99 μm lines; $14'' \times 27''$ for the 13.1–24.3 μm lines; and $20'' \times 33''$ for the 33.5 & 36.0 μm lines.

The position angle of the long-axis of the various apertures were 183.17, 13.27, 349.07, and 193.71° for NGC 2022, NGC 6210, NGC 6818, and IC 2165, respectively, and a rough estimate of the respective "diameters" are 19″, 16.2″, 20″, and 9″. However, there is certainly emission well beyond these "diameters" in the case of NGC 6210 and NGC 6818—see an overlay of our *ISO* apertures on *HST*/WFPC2 images taken by us under GO-6792 and other WFPC2 images under GO-6792[5].

The best object for our analysis in this sense is IC 2165, which is smaller than the smallest aperture. For the other PNs, the use of line flux ratios may still be valid as long as the specific ionic emitting zone is circumscribed by the smaller of the two apertures. Of the six line sets, *only* the [Ne V] pair of lines (14.3, 24.3) were observed with the same aperture size.

Figs. 3 and 4 are *ISO* SWS02 spectra of the

[5]Available as ∼rubin/turtle.html and ∼rubin/zorro.html from the web server http://www-space.arc.nasa.gov/

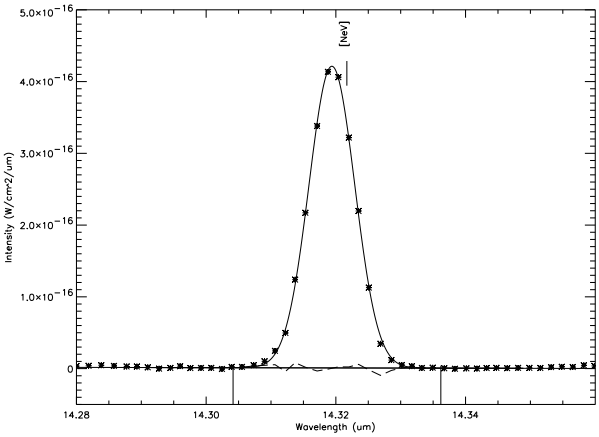

Fig. 3. ISO SWS02 spectrum of [Ne V] 14.32 μm line in the PN NGC 6818. This important N_e-diagnostic line cannot be observed even from an airborne platform. The data (asterisks) have been fit with a Gaussian and a linear baseline. The residuals, data point minus curve fit, are indicated as the dashed line.

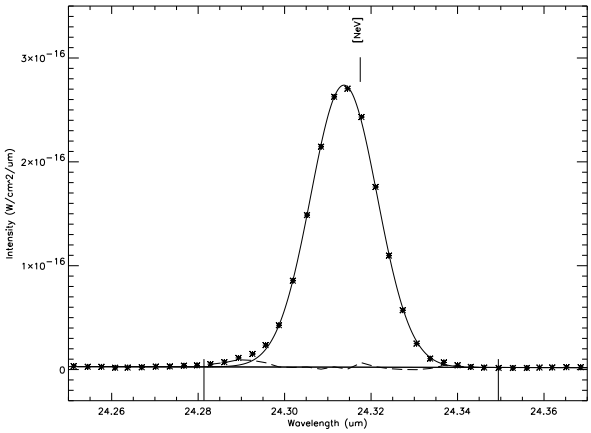

Fig. 4. Similar to Fig. 3 for the ISO SWS02 spectrum of [Ne V] 24.32 μm line in the PN NGC 6818.

[Ne V] 14.32 and 24.32 μm lines in NGC 6818. The aperture used for each was $14'' \times 27''$. The data are fit very well by a Gaussian profile. Data processing was performed using the ISO Spectral Analysis Package (ISAP). NGC 6818 is not fully enclosed by a $14'' \times 27''$ aperture. However, the same portion of the nebula is observed in both of these lines. Because the high ionization Ne^{+4} zone is much more concentrated toward the central star than the full ionized (H II) region is, it is highly probable that the entire Ne^{+4} zone is enclosed within the observed aperture.

Figure 5 shows the theoretical flux ratio $F(14.3)/F(24.3)$ vs. N_e (cm^{-3}), using collision strengths from Lennon & Burke (1994). Our *ISO* data with regard to this ionic species are most interesting. In the subsections to follow, we present the

Ionized Gaseous Nebulae (Mexico City, 21-24 November 2000)
Editors: William Henney, José Franco, Marco Martos, & Miriam Peña

SWS data and discuss the six ionic species in order of lowest to highest degree of ionization as indicated by the range in ionization potential (I.P.) over which the species exist.

3.1. *S III*

Observations were made of both the [S III] 18.7 and 33.5 μm lines in all four of our program PNs. The line profiles were fit with the line-fitting routine in ISAP, which provides the line flux and uncertainty. We fit the data points with a Gaussian and a linear baseline such as shown in Figs. 3 and 4 for the [Ne V] data. In general, the data were fit well by this method. Table 1 presents the measured fluxes and uncertainties. These uncertainties do not include systematic errors. The last column has the $N_{\rm e}$ derived from the flux ratio assuming a $T_{\rm e}$ of 10 000 K. It is likely that only the $N_{\rm e}$ for IC 2165 is valid. For the others, because of the extended [S III] emission and the mismatch of aperture sizes, the F(18.7)/F(33.5) ratio is likely a lower limit and the $N_{\rm e}$ entry a lower limit.

In the lower part of Table 1, we provide the theoretical $F(18.7)/F(33.5)$ ratio in the low-$N_{\rm e}$ limit; there, the smallest value of the ratio obtains. The transitions are shown in a term diagram (not to scale) with $N_{\rm crit}$-values for levels 2 and 3 for $T_{\rm e}$ = 10 000 K.

3.2. *Ar III*

Observations were made of both the [Ar III] 8.99 and 21.8 μm lines in NGC 6210 and NGC 6818. Table 2 presents the measured fluxes for these data. The comments regarding line fitting, etc., and the tabular entries that accompanied Table 1 apply here and for the ionic species to follow. In the lower part of the table, we have the theoretical $F(21.8)/F(8.99)$ ratio in the low-$N_{\rm e}$ limit, where the highest value of the ratio obtains. For NGC 6210, the observed ratio is close to the low-$N_{\rm e}$ asymptotic limit, where the ratio is insensitive to $N_{\rm e}$ and thus not useful for deriving $N_{\rm e}$. For this and other such instances, "near low limit" is entered in the $N_{\rm e}$-column of the Table. For NGC 6818, the observed ratio exceeds the low-$N_{\rm e}$ limit for any reasonable $T_{\rm e}$. Because the [Ar III] emission is likely more extended than the smaller $14''\times20''$ aperture, the $F(21.8)/F(8.99)$ ratio is likely an upper limit and thus any inference that the observed ratio is *out of the theoretical bounds* is uncertain. We enter "XXX low ?" in the table.

3.3. *Ne III*

Observations were made of both the [Ne III] 15.5 and 36.0 μm lines in IC 2165, NGC 6210, and NGC 6818. Table 3 presents the measured fluxes for these data as well as the theoretical F(36.0)/F(15.5) ratio in the low-$N_{\rm e}$ limit, where the highest value of the ratio obtains. For each, the observed ratio exceeds the low-$N_{\rm e}$ limit. However, because the [Ne III] emission may be more extended than the smaller $14'' \times 27''$ aperture for NGC 6210 and NGC 6818, the F(36.0)/F(15.5) ratio is likely an upper limit and again have an uncertain (XXX low ?) conclusion. On the other hand, for IC 2165, we are dealing with integrated fluxes and conclude robustly that the observed ratio is *out of the theoretical bounds* and enter "XXX low" in the table. The theoretical ratio in the

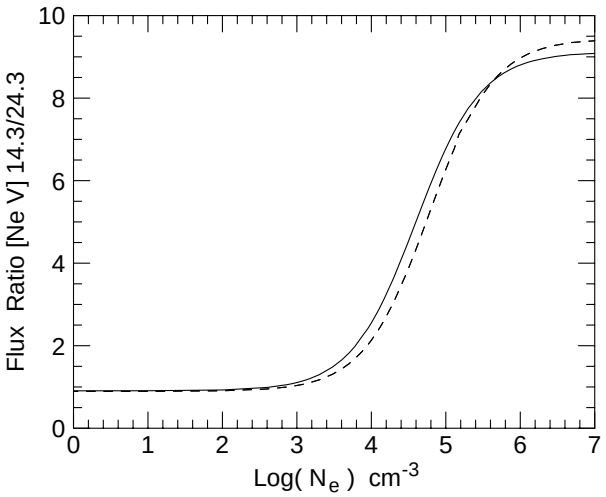

Fig. 5. An outstanding indicator of $N_{\rm e}$ is the flux ratio of [Ne V] (14.3/24.3). This shows the theoretical flux ratio F(14.3)/F(24.3) vs. $N_{\rm e}$ (cm^{-3}). The ratio is insensitive to $T_{\rm e}$ (10 000 K solid, 15 000 K dashed curve). This diagnostic is now available from ISO data.

TABLE 1

[S III] – I.P. range 23.33 – 34.83 eV

Source	F(18.7) (W cm^{-2})	F(33.5)	F(18.7)/F(33.5)	N_e (cm^{-3})*
IC2165	4.879E-19 ±7.656E-21	2.048E-19 ±1.747E-20	2.382	3130
NGC2022	1.561E-19 ±8.529E-21	1.659E-19 ±8.633E-21	0.941	573
NGC6210	2.196E-18 ±3.221E-20	1.111E-18 ±3.473E-20	1.977	2340
NGC6818	1.475E-18 ±2.014E-20	1.326E-18 ±3.181E-20	1.112	844

* for T_e = 10,000 K.

****

Theoretical Ratio in Low-N_e Limit: lowest value at low-N_e limit

T_e (K)	Ratio
10,000	0.6084
15,000	0.6815
20,000	0.7378

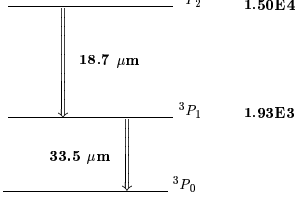

TABLE 2

[Ar III] – I.P. range 27.63 – 40.74 eV

Source	F(8.99) (W cm^{-2})	F(21.8)	F(21.8)/F(8.99)	N_e (cm^{-3})
NGC6210	9.676E-19 ±1.754E-20	6.478E-20 ±6.777E-21	0.0670	near low limit
NGC6818	5.465E-19 ±1.349E-20	4.806E-20 ±6.682E-21	0.0880	XXX low ?

****

Theoretical Ratio in Low-N_e Limit: highest value at low-$N_{e_{lim}}$ limit

T_e (K)	Ratio	N_{crit} (cm^{-3})
10,000	0.0680	
15,000	0.07037	
20,000	0.07197	

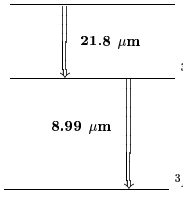

TABLE 3

[Ne III] – I.P. range 40.96 – 63.45 eV

Source	F(15.5) (W cm^{-2})	F(36.0)	F(36.0)/F(15.5)	N_e (cm^{-3})
IC2165	3.130E-18 ±3.031E-20	3.097E-19 ±6.295E-21	0.0989	XXX low
NGC6210	1.614E-17 ±2.700E-19	1.666E-18 ±6.222E-20	0.1032	XXX low ?
NGC6818	4.852E-18 ±3.896E-20	7.057E-19 ±1.629E-20	0.1454	XXX low ?

****

Theoretical Ratio in Low-N_e Limit: highest value at low-$N_{e_{lim}}$ limit

T_e (K)	Ratio	N_{crit} (cm^{-3})
10,000	0.0879	
15,000	0.0873	
20,000	0.0860	

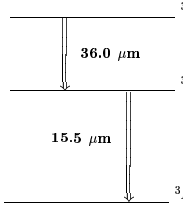

TABLE 4

[Ar V] – I.P. range 59.81 – 75.04 eV

Source	F(7.90) (W cm^{-2})	F(13.1)	F(7.90)/F(13.1)	N_e (cm^{-3})
IC2165	5.954E-20 ±3.904E-21	9.748E-20 ±1.844E-20	0.611	near low limit
NGC6818	1.057E-19 ±1.891E-21	1.833E-19 ±4.826E-21	0.577	near low limit

****

Theoretical Ratio in Low-N_e Limit: lowest value at low-N_e limit

T_e (K)	Ratio	N_{crit} (cm^{-3})
10,000	0.5727	
15,000	0.6136	
20,000	0.6413	

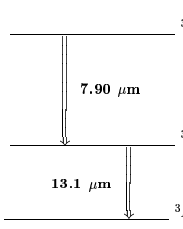

TABLE 5

[Ne V] – I.P. range 97.11 – 126.21 eV

Source	F(14.3) (W cm^{-2})	F(24.3)	F(14.3)/F(24.3)	N_e (cm^{-3})
IC2165	2.284E-18 ±3.838E-20	1.957E-18 ±1.844E-20	1.167	1300*
NGC2022	1.319E-18 ±1.982E-20	1.596E-18 ±2.108E-20	0.827	XXX low
NGC6818	3.701E-18 ±3.384E-20	5.233E-18 ±5.306E-20	0.707	XXX low

* for T_e = 10,000; 1950 cm^{-3} at 15,000 K.

****

Theoretical Ratio in Low-N_e Limit: lowest value at low-N_e limit

T_e (K)	Ratio	N_{crit} (cm^{-3})
10,000	0.9067	
15,000	0.8935	
20,000	0.8814	
25,000	0.8712	

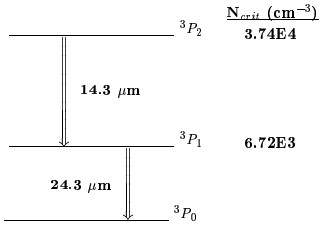

TABLE 6

[Mg V] – I.P. range 109.31 – 141.27 eV

Source	F(5.61) (W cm^{-2})	F(13.5)	F(13.5)/F(5.61)	N_e (cm^{-3})
IC2165	2.692E-19 ±9.792E-21	2.779E-20 ±4.807E-21	0.1032	XXX low

****

Theoretical Ratio in Low-N_e Limit: highest value at low-$N_{e_{lim}}$ limit

T_e (K)	Ratio	N_{crit} (cm^{-3})
10,000	0.0797	
15,000	0.0814	
20,000	0.0819	

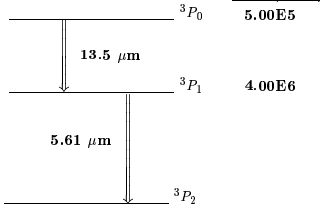

low-N_e limit is set by the effective collision strengths (CS). Perhaps the data for IC 2165 are pointing to a need to reexamine the CS, particularly those between the ^3P fine-structure levels.

3.4. *Ar V*

Observations were made of both the [Ar V] 7.90 and 13.1 μm lines in IC 2165 and NGC 6818. Table 4 presents the measured fluxes for these data as well as the theoretical $F(7.90)/F(13.1)$ ratio in the low-N_e limit, where the lowest value of the ratio obtains. For both PNs, the observed ratio is near the low-N_e limit. Here, even in the case of NGC 6818, it is likely that the Ar^{+4} zone is much more centrally concentrated than the size of the H^+ zone; but if the [Ar V] 7.90 emission were more extended than the smaller $14'' \times 20''$ aperture used, then the $F(7.90)/F(13.1)$ ratio would be a lower limit.

3.5. *Ne V*

Observations were made of both the [Ne V] 14.3 and 24.3 μm lines in IC 2165, NGC 2022, and

Ionized Gaseous Nebulae (Mexico City, 21-24 November 2000)
Editors: William Henney, José Franco, Marco Martos, & Miriam Peña

NGC 6818 (see Figs. 3 and 4). Table 5 has the measured fluxes for these data as well as the theoretical $F(14.3)/F(24.3)$ ratio in the low-N_e limit, where the lowest value of the ratio obtains. For NGC 6818, the observed ratio is well below the low-N_e theoretical limit for any reasonable T_e; for NGC 2022, the observed ratio is also out of bounds. For IC 2165, we derive $N_e = 1300$ and 1950 cm^{-3} from Fig. 5 (see Table 5). Compared to N_e-values derived for IC 2165 by Stanghellini & Kaler (1989), albeit for other ions, the values here are very low.

We are aware of three other measurements of N_e from the [Ne V] ratio using ISO data. Alexander et al. (1999) found an observed ratio that is close to the low-N_e limit for the Seyfert galaxy NGC 4151. For the PNs NGC 7027 and NGC 6302, van Hoof et al. (2000), found N_e of 26 900 and 12 300 cm^{-3} using $T_e \sim 20\,000$ K. Compared to N_e-values derived from optical data for these PNs for other ions (Stanghellini & Kaler 1989), again their values are lower. The fact that these previously published [Ne V] ratios and our new IC 2165 result yield generally lower N_e-values than other methods tends to lend support to our conclusion that the low-N_e theoretical limit may need reexamination per our "XXX low" results. Just because the NGC 7027, NGC 6302, and IC 2165 data lead to "legal, in-theoretical-bounds values" does not mean the inferred N_es are correct and does not rule out the possibility that the collision strengths between the ^{3}P levels may need revision.

3.6. *Mg V*

Observations were made of both the [Mg V] 5.61 and 13.5 μm lines in IC 2165. In Table 6 are the measured fluxes as well as the theoretical $F(13.5)/F(5.61)$ ratio in the low-N_e limit, where the highest value of the ratio obtains. Again, the observed ratio is out of the theoretical bounds.

4. SUMMARY AND CONCLUSIONS

There are several instances of the observed line flux ratio being clearly out of range of the theoretical predictions using current atomic data. This is most dramatically illustrated with the [Ne V] (14.3/24.3) flux ratio for NGC 6818. These are both strong lines observed with signal-to-noise better than 100. The observed flux ratio is 0.707, which is significantly less than the predicted ratio using collision strengths from Lennon & Burke (1994). Because the line ratio near the low-N_e limit depends on collision strengths and *not* the A-values, this result may point toward a need to reexamine the collision strengths.

As this work shows, progress in the future will also depend very much on the ability to obtain cospatial observations of the line pairs in the IR used as an N_e diagnostic. Thus it is important that future astronomical facilities be able to do this and maintain a level of flux calibration sufficient for analyses of electron density, such as we had hoped to perform.

This research was supported by NASA through data analysis grants to the ISO General Observer program and by AURA/STScI grant related to GO-6792. We made use of Richard Shaw's program at http://ra.stsci.edu/nebular/ionic.html for several of the ions.

REFERENCES

Alexander, T., et al. 1999, ApJ, 512, 204
Burkert, A., & O'Dell, C. R. 1998, ApJ, 503, 792
Henney, W. J., & O'Dell, C. R. 1999, AJ, 118, 2350
Henry, R. B. C., & Worthey, G. 1999, PASP, 111, 919
Kwitter, K. B., & Henry, R. B. C. 1998, ApJ, 493, 247
Lennon, D. J., & Burke, V. M. 1994, A&AS, 103, 273
Liu, X.-W. 1998, MNRAS, 295, 699
Liu, X.-W., Storey, P. J., Barlow, M. J., & Clegg, R. E. S. 1995, MNRAS, 272, 369
Liu, X.-W., Storey, P. J., Barlow, M. J., Danziger, I. J., Cohen, M. & Bryce, M. 2000, 312, 585
Peimbert, M. 1967, ApJ, 150, 825
Rubin, R. H. 1989, ApJS, 69, 897
Rubin, R. H., Simpson, J. P., Lord, S. D., Colgan, S. W. J., Erickson, E. F., & Haas, M. R. 1994, ApJ, 420, 772
Shaver, P. A., McGee, R. X., Newton, L. M., Danks, A. C., & Pottasch, S. R. 1983, MNRAS, 204, 53
Simpson, J. P., Colgan, S. W. J., Rubin, R. H., Erickson, E. F., & Haas, M. R. 1995, ApJ, 444, 721
Stanghellini, L. & Kaler, J. B. 1989, ApJ, 343, 811
van Hoof, P. A. M., Beintema, D. A., Verner, D. A., & Ferland, G. J. 2000, A&A, 354, L41
Viegas, S. M., & Clegg, R. E. S. 1994, MNRAS, 271, 993
Walsh, J. R., & Meaburn, J. 1993, The Messenger, 73, 35

R. H. Rubin: NASA/Ames Research Center, MS 245-6, Moffett Field, CA 94035-1000, USA, (rubin@cygnus.arc.nasa.gov).